Noise beating in hybrid phase-sensitive amplifier systems

B. Corcoran,[1,2] R. Malik,[1] S. L. I. Olsson,[1] C. Lundström,[1] M. Karlsson,[1] and P. A. Andrekson[1,*]

[1]*Fiber Optic Communication Research Centre (FORCE), Dept. Microtechnology and Nanoscience, Chalmers University of Technology, Gothenburg 412 96, Sweden*
[2]*Now with: Centre for Ultrahigh-bandwidth Devices for Optical Systems (CUDOS), Dept. Electrical and Computer Systems Engineering, Monash University, Clayton 3168, Australia*
[*]*peter.andrekson@chalmers.se*

Abstract: We investigate the effect of noise loading in a hybrid phase-sensitive amplifier system, analyzing the effect of noise beating between the signal and idler waves coupled in a parametric amplifier. Through analyzing input and output optical signal to noise ratios, we find that system performance of a phase-sensitive amplifier is 3 to 6 dB improved over a phase-insensitive amplifier, depending on the ratio of loaded noise power to that of vacuum fluctuations.

OCIS codes: (060.2320) Fiber optics amplifiers and oscillators; (190.4970) Parametric amplifiers and oscillators; (190.4380) Nonlinear optics, four-wave mixing

References and links

1. C. M. Caves, "Quantum limits on noise in linear amplifiers," Phys. Rev. D **26**, 1817–1839 (1982).
2. A. Mosset, F. Devaux, and E. Lantz, "Spatially noiseless optical amplification of images," Phys. Rev. Lett. **94**, 223603 (2005).
3. S.-K. Choi, M. Vasilyev, and P. Kumar, "Noiseless optical amplification of images," Phys. Rev. Lett. **18**, 1938–1941 (1999).
4. J. A. Levenson, I. Abram, T. Rivera, P. Fayolle, J. C. Garreau, and P. Grangier, "Quantum optical cloning amplifier," Phys. Rev. Lett. **70**, 267–270 (1993).
5. M. Asobe, T. Umeki, and O. Tadanaga, "Phase sensitive amplification with noise figure below the 3 dB quantum limit using CW pumped PPLN waveguide," Opt. Express **20**, 13164–13172 (2012).
6. Z. Tong, C. Lundström, P. A. Andrekson, M. Karlsson, and A. Bogris, "Ultralow noise, broadband phase-sensitive optical amplifiers, and their applications," J. Sel. Top. Quantum Electron. **18**, 1016–1032 (2011).
7. T. Umeki, M. Asobe, H. Takara, Y. Miyamoto, and H. Takenouchi, "Multi-span transmission using phase and amplitude regeneration in PPLN-based PSA," Opt. Express **21**, 18170–18177 (2013).
8. B. Corcoran, S. L. I. Olsson, C. Lundström, M. Karlsson, and P. Andrekson, "Phase-sensitive optical pre-amplifier implemented in an 80km DQPSK link," in *Proc. OFC 2012* (2012), PDP5A.
9. K. J. Lee, F. Parmigiani, S. Liu, J. Kakande, P. Petropoulos, K. Gallo, and D. Richardson, "Phase sensitive amplification based on quadratic cascading in a periodically poled lithium niobate waveguide," Opt. Express 17, 20393–20400 (2009).
10. B. J. Puttnam, D. Mazroa, S. Shinada, and N. Wada, "Large phase sensitive gain in periodically poled lithium niobate with high pump power," Photonics Technol. Lett. **23**, 426–428 (2011).
11. J. A. Levenson, I. Abram, T. Rivera, and P. Grangier, "Reduction of quantum noise in optical parametric amplification," J. Opt. Soc. Am. B **10**, 2233–2238 (1993).
12. D. Lovering, J. Webjörn, P. Russell, J. Levenson, and P. Vidakovic, "Noiseless optical amplification in quasi-phase-matched bulk lithium niobate," Opt. Lett. **21**, 1439–1441 (1996).
13. R. Tang, J. Lasri, P. S. Devgan, V. Grigoryan, P. Kumar, and M. Vasilyev, "Gain characteristics of a frequency nondegenerate phase-sensitive fiber-optic parametric amplifier with phase self-stabilized input," Opt. Express **13**, 10483–10493 (2005).

#202454 - $15.00 USD Received 3 Dec 2013; revised 20 Jan 2014; accepted 24 Jan 2014; published 5 Mar 2014

14. R. Slavík, A. Bogris, F. Parmigiani, J. Kakande, M. Westlund, M. Sköld, L. Grüner-Nielsen, R. Phelan, D. Syvridis, P. Petropoulos, and D. J. Richardson, "Coherent all-optical phase and amplitude regenerator of binary phase-encoded signals," J. Sel. Top. Quantum Electron. *18*, 859–869 (2012).
15. T. Umeki, H. Takara, Y. Miyamoto, and M. Asobe, "3-dB signal-ASE beat noise reduction of coherent multi-carrier signal utilizing phase sensitive amplification," Opt. Express **20**, 24727–24734 (2012).
16. T. Umeki, O. Tadanaga, M. Asobe, Y. Miyamoto, and H. Takenouchi, "First demonstration of high-order QAM signal amplification in PPLN-based phase sensitive amplifier," in *Proc. ECOC 2013* (2013), PDP1.C5.
17. Z. Tong, A. Bogris, C. Lundström, C. J. McKinstrie, M. Vasilyev, M. Karlsson, and P. A. Andrekson, "Modeling and measurement of the noise figure of a cascaded non-degenerate phase-sensitive parametric amplifier," Opt. Express *18*, 14820–14835 (2010).
18. C. McKinstrie, M. Karlsson, and Z. Tong, "Field-quadrature and photon-number correlations produced by parametric processes," Opt. Express **18**, 19792–19823 (2010).
19. C. Lundström, R. Malik, L. Grüner-Nielsen, B. Corcoran, S. L. I. Olsson, M. Karlsson, and P. A. Andrekson, "Fiber optic parametric amplifier with 10-dB net gain without pump dithering," Photonics Technol Lett. **25**, 234–237 (2013).
20. S. Olsson, B. Corcoran, C. Lundström, E. Tipsuwannakul, S. Sygletos, A. Ellis, Z. Tong, M. Karlsson, and P. Andrekson, "Injection locking-based pump recovery for phase-sensitive amplified links," Opt. Express **21**, 14512–14529 (2013).
21. X. Liu, S. Chandrasekhar, P. Winzer, A. Chraplyvy, R. Tkach, B. Zhu, T. Taunay, M. Fishteyn, and D. DiGiovanni, "Scrambled coherent superposition for enhanced optical fiber communication in the nonlinear transmission regime," Opt. Express **20**, 19088–19095 (2012).
22. Z. Tong, A. Bogris, M. Karlsson, and P. A. Andrekson, "Full characterization of the signal and idler noise figure spectra in single-pumped fiber optical parametric amplifiers," Opt. Express **18**, 2884–2893 (2010).
23. M. E. Marhic, G. Kalogerakis, K. K.-Y. Wong, and L. G. Kazovsky, "Pump-to-signal transfer of low-frequency intensity modulation in fiber optical parametric amplifiers," J. Lightwave Technol. **23**, 1049–1055 (2005).
24. T. Richter, B. Corcoran, S. L. I. Olsson, C. Lundström, M. Karlsson, C. Schubert, and P. A. Andrekson, "Experimental characterization of a phase-sensitive four-mode fiber-optic parametric amplifier," in *Proc. ECOC 2012* (2012), Th.1.F.1.
25. Z. Tong, A. Wiberg, E. Myslivets, B. Kuo, N. Alic, and S. Radic, "Broadband parametric multicasting via four-mode phase-sensitive interaction," Opt. Express **20**, 19363–19373 (2012).
26. G. Lei and M. Marhic, "Performance investigation of a hybrid fiber optical parametric amplifier," Opt. Express **21**, 21932–21940 (2013).

1. Introduction

Phase-sensitive (PS) amplification is predicted to provide ideal 0 dB noise figure (NF) amplification [1]. In practice, phase-sensitive amplifiers (PSAs) are generally implemented through a nonlinear wave-mixing interaction, either in $\chi^{(2)}$ or $\chi^{(3)}$ nonlinear media. There have been several demonstrations of PSAs for low-noise amplification, for imaging [2,3], quantum optics [4], and optical communication systems [5–8]. Key to the achievement of low-noise amplification in these systems is the beating of waves at separate optical frequencies through nonlinear wave mixing, such as sum/difference frequency generation (SFG/DFG) [7, 9, 10], second harmonic generation (SHG) [2, 3, 5, 11, 12] and four wave mixing (FWM) [6, 8, 13]. In a PSA with high gain, this interaction can be modeled as a coherent summation of the fields at these separate frequencies (in the low gain regime, the separate waves are scaled before summation). As such, in-phase components between these mixing waves add constructively, while out-of-phase components beat destructively. For deterministic, correlated signals on these waves, these systems can be tuned to provide constructive addition. However, for uncorrelated, stochastic components, such as independent noise sources, the addition is incoherent. Effectively half the noise will add constructively whilst the other half cancels destructively. This difference between the beating of correlated signal and un-correlated noise components gives rise to the low-noise amplification achievable in PSAs.

PSAs in the optical domain to date have been achieved in two ways, beating a signal wave with waves locked into a single quadrature [7, 14, 15], or by beating the signal wave with a copy of itself [6, 13, 16]. The former method, employed in both SHG and frequency degenerate idler systems (utilizing either SFG or FWM), limits the signal wave to the phase axis defined

#202454 - $15.00 USD Received 3 Dec 2013; revised 20 Jan 2014; accepted 24 Jan 2014; published 5 Mar 2014

by these waves. Although these systems can provide low-noise amplification [7, 15], they limit the usable modulation formats in an optical communication system, where multi-level phase encoded signals are of interest. To date, the only PSA systems that can be considered modulation format independent are those where the signal beats with a copy of itself, as the signal essentially provides it's own phase reference in the copy. These type of systems have been implemented by copying the original signal to the idler wavelength in a phase-insensitive (PI) parametric amplifier, before launch into a second parametric amplifier which then operates as a PSA. We call such systems 'copier-PSAs', which have been extensively investigated using fiber optic parametric amplifiers (FOPAs) in terms of low-noise amplification [6].

In previous investigations, the low NF of these amplifiers can be seen to be a consequence of beating between vacuum fluctuations at the input to the PSA stage, while the correlated signal and idler are added constructively [17, 18]. However, this is not necessarily the situation one might have in a PSA amplified optical communication link. The only demonstration of PSA for long haul communication links utilizes a joint PSA-EDFA amplification scheme [7], and there may be further link NF advantages to harnessing distributed Raman amplification in copier-PSA systems to further reduce overall link NF [6]. However, in either Raman or EDFA hybrid PSA systems, it is possible that the noise present at the input of the PSA will not be dominated by vacuum fluctuations, but by spontaneous emission from other amplifiers.

In this paper we investigate the effect of optical noise in a copier-PSA system, through noise loading of the signal and idler waves with a varied level of ASE. We show that a 3 dB optical signal-to-noise ratio (OSNR) improvement is expected when amplifying with a PSA compared to amplifying with a PIA, where the loaded noise power is well above the vacuum level. Measurements show that this improvement in OSNR translates into a sensitivity improvement when measuring the bit error rate (BER) of QPSK signals, implying a real improvement in signal SNR. When reducing the loaded noise power at the PSA input to below the vacuum level, the OSNR difference shifts from 3 dB to 6 dB, consistent with our theoretical predictions. The implications of these results for hybrid PSA-PIA systems are then discussed.

2. Theory

FOPAs can be modeled semi-classically as lumped amplifiers using a matrix formalism as per [17]. The input and output fields at two the signal and idler frequencies (denoted below by the subscript $x = sig, idl$) of a FOPA can then be written as:

$$\begin{bmatrix} E_{sig,out} \\ E^*_{idl,out} \end{bmatrix} = \begin{bmatrix} \mu & \nu \\ \nu^* & \mu^* \end{bmatrix} \begin{bmatrix} E_{sig,in} \\ E^*_{idl,in} \end{bmatrix} \tag{1}$$

Here μ and ν are complex gain coefficients of the amplifier [17,18], which scale the field by $\sqrt{G}$ and $\sqrt{G-1}$ respectively, where G denotes power gain. The conjugation operators (*) denote a phase conjugation of either the gain coefficients or the fields. Note in this representation, as established in [17, 18], that the idler at both input and output of this matrix are the conjugate of the actual idler fields into and out of the FOPA. We can break down the fields at the two separate optical frequencies into a signal component (A_x) and a noise component (n_x). If the signal-to-noise ratio (SNR) into the FOPA is sufficiently high (i.e. if the input signal is shot noise limited), and pump relative intensity noise (RIN) is small enough, then the dominant noise term will be from vacuum fluctuations. Vacuum field fluctuations can be characterized as having zero mean and a power spectral density (S) at a given frequency (ν) of $S = h\nu/2$. Taking the noise over a reference bandwidth of 0.1 nm at a central wavelength of 1550 nm (i.e. as per convention for optical SNR), then the vacuum noise power can be calculated as:

$$P_{vac}|_{\delta\lambda=0.1nm} = h\nu/2 \cdot \delta\nu = 0.8nW = -61dBm \tag{2}$$

#202454 - $15.00 USD Received 3 Dec 2013; revised 20 Jan 2014; accepted 24 Jan 2014; published 5 Mar 2014

This vacuum limit then defines where vacuum fluctuations dominate over any noise added onto the signal and idler waves. The noise field term can then be split into two components, $n_{x,vac}$ for the vacuum noise and $n_{x,load}$ for loaded noise. In a copier-PSA system, the idler from the copier stage launched into the second 'PSA' FOPA is such that $A_{idl} = A^*_{sig}$. If we assume that both signal and idler have a sufficiently high SNR, the average power ($\langle E_x \rangle$, where $\langle\rangle$ denotes the average) is the mean squared magnitude of the signal field component (i.e. $\left\langle |A_x|^2 \right\rangle$) and the dominant noise term ($\sigma^2(E_x) = \left\langle |E_x|^2 \right\rangle - |\langle E_x \rangle|^2$) is from signal-noise beat variance, and proportional to the variance of n_x, i.e. $\sigma^2(E_x) \propto \sigma^2(n_x)$. The noise components $n_{x,vac}$ and $n_{x,load}$ are independent, so the the noise variance can be taken as $\sigma^2(n_x) = \sigma^2(n_{x,vac}) + \sigma^2(n_{x,load})$. Each of the noise variance terms can be taken as having a power spectral density, which can be normalized to a set bandwidth to provide a figure for power as in Eq. (2), such that the noise power is $P_{x,noise}|_{\delta\lambda=0.1nm} = P_{vac}|_{\delta\lambda=0.1nm} + P_{x,load}|_{\delta\lambda=0.1nm}$. With these assumptions, the signal-to-noise ratio (SNR) is then proportional to the OSNR, and can be found as:

$$OSNR_x = \left\langle |A_x|^2 \right\rangle / \left(P_{vac}|_{\delta\lambda=0.1nm} + P_{x,load}|_{\delta\lambda=0.1nm} \right) \tag{3}$$

Assuming high gain in the second FOPA (i.e. $G \approx G - 1$), the output field at the signal wavelength can then be written as:

$$E_{sig,out} = \sqrt{G}\left[\left(A_{sig} + n_{sig,load} + n_{sig,vac} \right) + \left(A^*_{sig} + n_{idl,load} + n_{idl,vac} \right)^* \right] \tag{4}$$

$$= \sqrt{G}\left[2A_{sig} + n_{sig,load} + n_{sig,vac} + n^*_{idl,load} + n^*_{idl,vac} \right] \tag{5}$$

This gives an OSNR at the output of the second FOPA (in PS mode) of:

$$OSNR_{sig,PSA} = 4|A_{sig}|^2 / \left(P_{sig,load} + P_{sig,vac} + P_{idl,load} + P_{idl,vac} \right) \tag{6}$$

When operating the second FOPA in PI mode, the idler is blocked before the FOPA through a large amount of attenuation in that waveband. While this means that we can take $A_{idl,in} = 0$ and $n_{idl,load} = 0$, the vacuum noise field is still present. As such the output field from the second FOPA can be taken as:

$$E_{sig,out} = \sqrt{G}\left[A_{sig} + n_{sig,load} + n_{sig,vac} + n^*_{idl,vac} \right] \tag{7}$$

Consequently, the OSNR at the output of the second FOPA (operating in PI mode) is given by:

$$OSNR_{sig,PIA} = |A_{sig}|^2 / \left(P_{sig,load} + P_{sig,vac} + P_{idl,vac} \right) \tag{8}$$

By comparing Eqs. (6) and (8), we can find the ratio of expected OSNRs out of the second FOPA when running in PI and PS modes (i.e. $\Delta OSNR$). If we assume the same noise loading on signal and idler waves, and that the difference in optical frequency between the two is much smaller than their central frequencies (i.e. $|(\nu_{sig} - \nu_{idl})| << \nu_{sig}$), then we find:

$$\Delta OSNR = 4\left(\frac{2 + P_{load}/P_{vac}}{2 + 2 \cdot P_{load}/P_{vac}} \right) \tag{9}$$

Equation (9) shows that the change in OSNR at output from the second FOPA is a factor of 4 (6 dB) where vacuum noise dominates (i.e. $P_{vac} >> P_{load}$), as measured previously [6]. At the other extreme, where the loaded noise is the dominant noise source (i.e. $P_{vac} << P_{load}$), $\Delta OSNR$ becomes 2 (3 dB). However, the factor of 4 in Eq. (9) is the ratio of signal power gain for the FOPA under test when comparing operating in PI and PS mode. Generally, this 6dB gain difference is not quite achieved, with the achievable range somewhere between 5-6 dB [6]. This can be due to a number of factors that prevent the PSA from operating ideally,

#202454 - $15.00 USD Received 3 Dec 2013; revised 20 Jan 2014; accepted 24 Jan 2014; published 5 Mar 2014

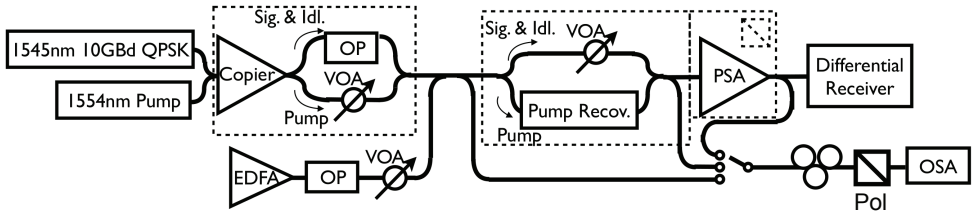

Fig. 1. Experimental set-up. Sections enclosed by dotted lines were removed for back-to-back tests. VOA: variable optical attenuator, Pol.: polarizer

such as misalignment of the interacting waves in polarization, time or phase, or non-idealities in the highly nonlinear fiber used (e.g. polarization mode dispersion, etc). In non-FOPA systems, limits to achievable gain can also change the gain PS/PI gain ratio away from 6 dB. To account for these non-idealities, we can more generally rewrite Eq. (9) as:

$$\Delta OSNR = \frac{G_{PSA}}{G_{PIA}} \left(\frac{2 + P_{load}/P_{vac}}{2 + 2 \cdot P_{load}/P_{vac}} \right) \tag{10}$$

This shows that in an unoptimized PSA system, where the ratio $G_{PSA}/G_{PIA} < 4$, in the high noise loading limit PSA provides less than 3dB benefit over a PIA system.

3. Experiment

In order to test the predictions just outlined, we can test the operation of a FOPA with inputs with various levels of noise loading. Figure 1 shows the experimental set-up used to vary the noise loading on signal and idler waves between copier and PSA stages. A 10 Gbd QPSK signal at 1545 nm is launched with a phase-modulated pump wave into the first 'copier' FOPA. The signal at input to the copier is >0 dBm, the pump wave provides <10 dB amplification. We estimate an OSNR of the signal and idler waves exiting the copier in excess of 50 dB. Signal and idler waves are balanced in power using an optical processor (OP - Finisar WaveShaper), then attenuated before mixing with ASE for noise loading. The loaded ASE is carved from the output of an EDFA with another OP in order to noise load only in the signal and idler wavebands. An equal amount of ASE is added to both wavebands to ensure the same loaded OSNR for each wave. The noise loaded waves are then launched into the second FOPA, which can be made to operate in PI or PS mode by blocking or passing, respectively, the idler waveband in the OPs. The OSNR at input and output of the second FOPA is analyzed by an optical spectrum analyser (OSA) after passing through a polarizer. The polarizer allows us to investigate the OSNR in the polarization of the signal only, which is ensured by peaking the signal power measured by the OSA by adjusting a polarization controller (PC) before the polarizer. In back-to-back tests, the second 'PSA' FOPA stage is replaced by a polarizer to emulate the effect of single polarization gain.

The FOPAs each consist of two germanium-doped highly nonlinear fibers (HNLFs), stretched along their length in order to suppress stimulated Brillouin scattering (SBS), joined with an optical isolator to further suppress SBS [19]. The pump, between the first and second FOPAs, is passed through a pump recovery system [20] (utilised for systems with a long fiber span between the FOPAs [8]) for convenience. When analyzing BER of the signal passed though this system, the signal is filtered out before passing into an amplified receiver. The signal is differentially detected, using a 1-bit delay line interferometer and balanced detector, with the

#202454 - $15.00 USD Received 3 Dec 2013; revised 20 Jan 2014; accepted 24 Jan 2014; published 5 Mar 2014

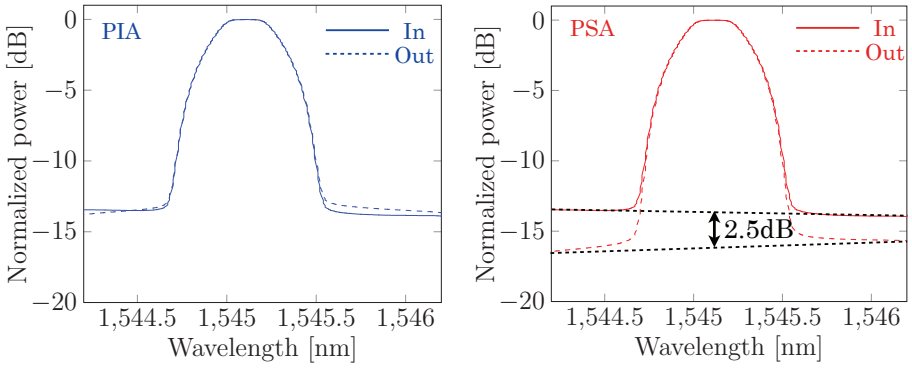

Fig. 2. Optical spectra at input (solid) and output (dashed) of the second FOPA, for both PI (left) and PS (right) operation. Resolution was set to 0.1 nm.

pattern analyzer programmed with a differential version of the transmitted 2^{15}-1 pattern length pseudo-random bit sequence (PRBS).

Figure 2 shows the single polarization optical spectra at input and output of the second FOPA with a high level of noise loading (input single polarization OSNR 14 dB), with the second FOPA operating in either PI or PS mode. In both modes, gain is kept to 21dB, and the power in the signal waveband at the FOPA input kept constant at -27dBm. In PI mode, the OSNR at the output is the same as at the input, and the additional noise added by the second FOPA is negligible compared to the loaded noise. However, when operating in PS mode, an OSNR improvement of 2.5 dB is observed comparing input to output, close to the 3 dB as predicted by Eq. (9).

Similar measurements are made for varied levels of loaded ASE power to the signal and idler wavebands. Figure 3 shows the measured values of OSNR at output of the second FOPA for various noise loaded powers (corresponding to different input OSNR values). For high noise loading (around 15 dB OSNR), the output OSNR when operating the second FOPA in PI mode tracks the input OSNR, while in PS mode, OSNR is improved by 2.5 dB. As the power of the loaded ASE decreases, output OSNR for both PI and PS mode is degraded compared to input OSNR. This is because the intrinsic noise from the second FOPA becomes significant compared to the loaded noise power and the output OSNR trends toward the value for a shot noise limited input. For a PI amplified signal, the output OSNR is expected to be $P_{sig,in}/2P_{vac}$ (blue dashed line, Fig. 3), as per Eq. (8), which here gives 31dB. At the output of a shot noise limited PSA, we expect the OSNR to be $4P_{sig,in}/2P_{vac}$ (red dashed line, Fig. 3) as per Eq. (6), which here is 37dB. Consequently, the difference in output OSNR of the FOPA running in PI and PS modes trends toward 5 dB, close to the 6 dB expected through Eq. (9).

By interpolating between the measured points in Fig. 3, we can compare the difference in output OSNRs operating in PI and PS mode for different amounts of ASE noise loading. Figure 4 shows the values of OSNR change comparing PI and PS mode from interpolating the measured data against the predicted curve from Eq. (10). The two theoretical curves use slightly different values for the ratio of PS to PI gain, the 5.5 dB difference corresponds to the measured gain difference when switching from PS to PI mode for the second FOPA. This curve relies only on the vacuum noise level, rather than any assumed extra noise factors (such as spontaneous Raman scattering, etc), and the difference in PI and PS mode gain. However, even with such a simple model, the measured data matches quite well to theory, indicating that treating vacuum

#202454 - $15.00 USD Received 3 Dec 2013; revised 20 Jan 2014; accepted 24 Jan 2014; published 5 Mar 2014

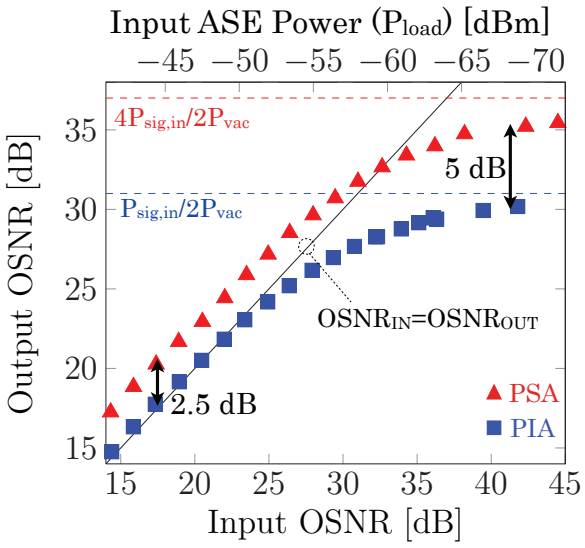

Fig. 3. Measured input and output OSNRs for various levels of noise loading between the two FOPAs, with the second FOPA operating in PI (blue squares) and PS (red triangles) modes. The solid black line is for equal input and output OSNRs, the dotted lines the expected value for output OSNR in the vacuum noise dominant regime. Input power in the signal waveband is a constant -27dBm.

noise as a dominant noise term in some situations can provide a good model of operation for FOPAs.

As pump noise transfer can be a significant effect in FOPA systems, it is important to check that the 2.5 dB OSNR gain measured in the noise loading dominant regime relates to an improvement in BER curves comparing PI to PS mode. Additionally, this allows us to compare FOPA performance in this regime against back-to-back results with noise loading only to ascertain if there are any detrimental effects on the signal when amplified by FOPAs. Figure 5 shows BER curves against received OSNR, with OSNR varied by varying the amount of noise loaded between the two FOPA stages (or directly between transmitter and receiver). In the back-to-back case, a polarizer was placed before the receiver to measure a single polarization, which is important when comparing to the FOPAs we use as they operate for a single polarization only. The back-to-back and PIA results line up well for the range of OSNRs investigated, which matches expectations in this regime. Figure 3 shows input OSNR matching output OSNR for the second FOPA in PI mode. When operating the second FOPA in PS mode, the system shows 2.7 dB greater sensitivity at the error free (BER=10^{-9}) level. This is slightly improved when compared with the increased OSNR in Fig. 3, however when making the BER measurements above, the gain difference PI/PS mode was measured to be slightly larger than previously measured.

Constellation diagrams of the signal also give a qualitative insight to the suppression of noise through beating. While intuitively one might imagine the noise being squeezed along the axes of signal phase, Fig. 6 shows a typical symmetrical Gaussian distribution of noise about the signal points. As mentioned in the introduction and highlighted in Eq. (4), the output of the PSA is a summation of the signal and idler fields. This leads to the direct addition of the Gaussian-like noise terms on each field to provide the symmetrical distribution observed, rather than being

#202454 - $15.00 USD Received 3 Dec 2013; revised 20 Jan 2014; accepted 24 Jan 2014; published 5 Mar 2014

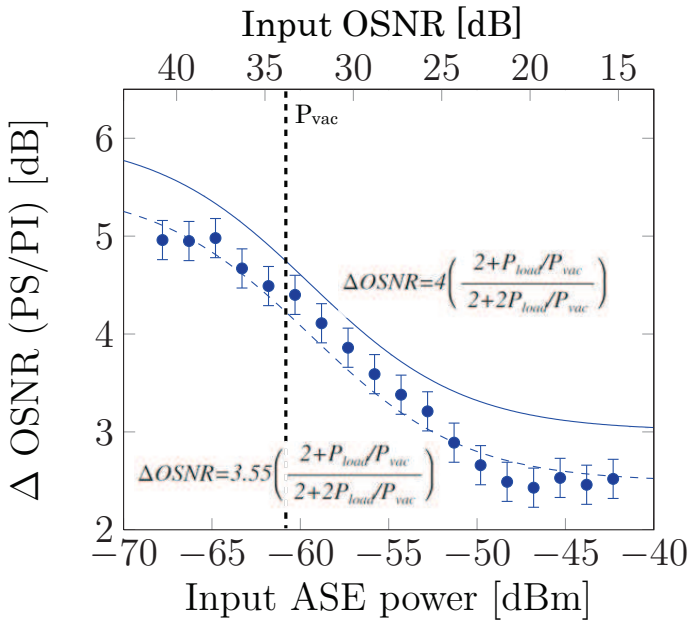

Fig. 4. Change in output OSNR of the second FOPA, PS/PI mode. The points represent change in OSNR interpolated from measured data, with the solid and dashed blue lines representing theoretical predictions for an ideal system and one with the measured 5.5dB PS/PI gain difference, respectively. Input power in the signal waveband is a constant -27dBm.

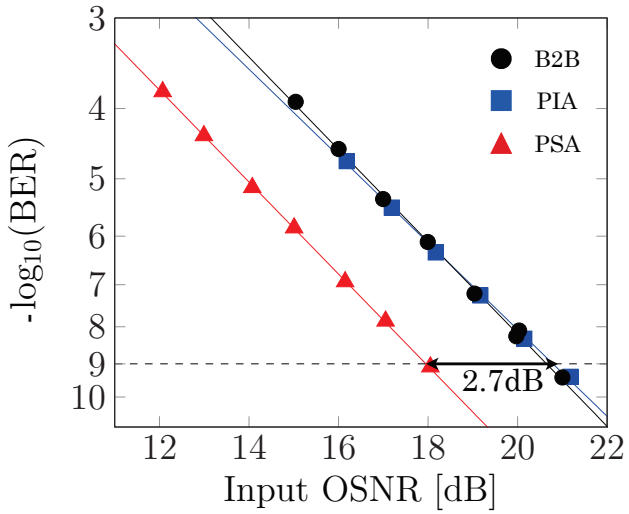

Fig. 5. BER curves at high noise loading.

#202454 - $15.00 USD Received 3 Dec 2013; revised 20 Jan 2014; accepted 24 Jan 2014; published 5 Mar 2014

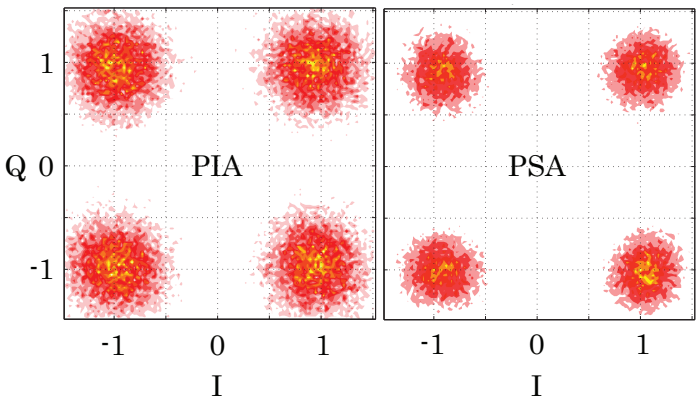

Fig. 6. Self-homodyne constellation measurements of the QPSK signal out of the PI and PS FOPAs for 15dB input OSNR.

squeezed along any particular phase axis. So in the case of Gaussian noise on signal and idler, the higher SNR of the PSA output should lead directly into an improvement in BER, as shown in Fig. 5.

4. Discussion

The close to 2.7 dB improvement of sensitivity for our ASE dominated hybrid system is quite similar to the ideally 3dB improvement expected with a system with simultaneous detection of two carriers modulated with the same data, as mentioned in [8, 21]. In the case of PSA here, both signal and idler have the same encoded data, but uncorrelated noise loaded on. In the high noise loading regime, the ideal sensitivity improvement is only 3 dB. As such, it can be argued that in the regime where loaded noise is the dominant noise source, that one could simply detect both signal and idler waves and process in the electronic domain [8, 21], instead of having to rely on optical methods to superimpose these two waves. As such, in a copier-PSA system operating in the noise loading regime, PSA does not provide appreciable benefit over a PIA scheme with two channels carrying the same data. This conclusion is particularly important for any potential copier-PSA system incorporating distributed Raman amplification (DRA) between copier and PSA, where it would be expected that DRA would have a similar effect to noise loading. As such, the benefit of adding DRA to a copier-PSA link as suggested in [6] may only be achievable if special consideration is given to noise when designing such a system.

Note that in the analysis presented here, the effect of pump RIN transfer noise is neglected. The effect can degrade the quality of optical signals amplified in both PI and PS FOPAs. The effect of this noise source has been well studied in PI FOPAs [22, 23], however, the specific effect of RIN on the system studied here remains open for further study.

To the best of our knowledge, beating signal and idler waves in a PSA is a unique way to achieve a higher OSNR on two widely separated optical frequencies with correlated data. The only other demonstrated method shown to reduce OSNR from input to output also utilizes a phase-sensitive amplifier [15], with signals restricted to one phase axis and spaced around 1*nm*. While the immediate applications for this effect are not necessarily clear, an all-optical system

#202454 - $15.00 USD Received 3 Dec 2013; revised 20 Jan 2014; accepted 24 Jan 2014; published 5 Mar 2014

with signal bandwidths in excess of those detectable through electronic means would benefit from this approach. Moreover, it is expected that the OSNR improvement will increase with the number of modes (i.e. number of mixed signal and idler waves), e.g. a 4-mode parametric system [24] should provide a factor of 4 increase in OSNR (i.e. 6 dB) in the noise loading regime. Simultaneously improving noise on many modes might find use in optical frequency comb applications [25].

Hybrid parametric amplifier systems, where a PIA is used in concert with a PSA, can be used to increase overall gain, which in a parametric amplifier can be practically limited by factors like the choice of non-linear media [7] or inter-channel cross-talk [26]. In degenerate idler PSA systems (such as [7]), the second pump wave is usually generated from mixing signal and idler, and then passed into a laser for injection locking. In such a system, the second pump wave can be significantly regenerated by this process, so there is no additional noise to beat with. In this case, noise loading of the type we investigate here has little bearing on the PSA noise performance. In a copier-PSA, the first amplifier in a link of this type is a PIA, however this is not used to overcome link loss, but primarily to generate the conjugate idler. The noise from this amplifier can be made small by placing a large loss between copier and PSA [6, 8, 17, 18]. As shown here, if a PIA (such as an EDFA or DRA) is used before the PSA in order to overcome link loss in copier-PSA system, noise loading near to or above the vacuum level clearly has an effect on amplifier performance.

5. Conclusion

We have investigated noise beating in a copier-PSA system. With significant noise loading, an increase in OSNR of the signal wave of 2.5 dB was measured, close to the 3 dB predicated improvement. However in this regime, the noise figure advantage of the PSA is similar to that of detecting two waves carrying the same data simultaneously (e.g. the signal and idler from the copier here) at the receiver. Conversely, if the noise loaded onto signal and idler is attenuated to below the vacuum noise limit, the PSA can provide up to a 6 dB benefit, with a measured value up to 5 dB here. A simple theory of the expected noise beating was presented, with the suppression of noise shown to be dependent on the ratio of PI to PS gain of the amplifier under test. This investigation is expected to have implications in the design of hybrid FOPA amplification systems.

Acknowledgments

This work is supported by the Swedish Research Council, by the European Research Council under grant agreement ERC-2011-AdG - 291618 PSOPA and by the K.A. Wallenberg Foundation.

#202454 - $15.00 USD Received 3 Dec 2013; revised 20 Jan 2014; accepted 24 Jan 2014; published 5 Mar 2014